Succinylated gelatin improves the theranostic potential of radiolabeled exendin-4 in insulinoma patients

Mijke Buitinga [1*], Tom Jansen [1], Inge van der Kroon [1], Wietske Woliner-van der Weg [1], Marti Boss [1], Marcel Janssen [1], Erik Aarntzen [1], Martin Béhé [2], Damian Wild [3], Eric Visser [1], Maarten Brom [1], Martin Gotthardt [1]

[1] *Department of Radiology and Nuclear Medicine, Radboudumc, Nijmegen, The Netherlands*

[2] *Center for Radiopharmaceutical Sciences ETH-PSI-USZ, Paul Scherrer Institute, 5232 Villigen, Switzerland*

[3] *Division of Nuclear Medicine, University Hospital Basel, Basel, Switzerland*

[*]**Corresponding author**

Dr. Mijke Buitinga

Department of Radiology and Nuclear Medicine

Radboud university medical centre

P.O. Box 9101, 6500 HB Nijmegen, The Netherlands

Mijke.Buitinga@radboudumc.nl

Word count: 5000

This work was supported by BetaCure (FP7/2014–2018, grant agreement 602812) and INNODIA (IMI2-JU, grant agreement 115797).

Short running title: Exendin-4 for insulinoma therapy

ABSTRACT

Being highly expressed in insulinomas, the glucagon-like peptide-1 receptor (GLP-1R) is a potential target for diagnosis, localization and treatment with the radiolabeled GLP-1R agonist exendin. Tracer accumulation in the kidneys, however, hampers accurate diagnostic visualization of pancreatic tissue and prohibits the therapeutic application of radiolabeled exendin for beta-cell-derived tumors. Therefore, we evaluated the ability of succinylated gelatin (Gelofusine) to reduce the renal accumulation of radiolabeled exendin in humans and we performed dosimetric calculations to estimate the maximum absorbed insulinoma dose that could be achieved when exendin would be used for peptide receptor radionuclide therapy.

Methods: Ten healthy volunteers received 50 MBq ^{111}In-exendin-4, in combination with Gelofusine or saline in a crossover design. SPECT/CT images were obtained after 24 hours. The procedure was repeated three weeks later. Uptake of ^{111}In-exendin was determined by drawing regions of interest around the kidneys and in the pancreas. Planar scintigraphic ^{111}In-exendin images of five insulinoma patients were used for dosimetry studies estimating the maximum insulinoma absorbed dose that could be achieved without causing radiotoxicity to other organs.

Results: Gelofusine reduced the renal accumulation of ^{111}In-exendin-4 with 18.1%, whereas the pancreatic uptake remained unchanged. In 3 out of 10 subjects, the kidney uptake was reduced to such an extent that the pancreatic tail could be better discriminated from the kidney signal. Dosimetric estimations suggested that the insulinoma absorbed dose ranges from 30.3–127.8 Gy. This dose could be further increased to maximally 156.1 Gy when Gelofusine would be used.

Conclusion: We have shown that Gelofusine can reduce the renal accumulation of ^{111}In-exendin-4 in humans. This reduction does not only allow more accurate qualitative and quantitative analyses of radiolabeled exendin uptake in the tail region

of the pancreas, but it also potentiates the safe delivery of a higher radiation dose to GLP-1R positive tumors for therapy.

Keywords: Exendin-4, kidney uptake, insulinoma, radionuclide therapy, dosimetry.

INTRODUCTION

Insulinomas are rare neuroendocrine tumors arising from pancreatic beta-cells (*1*). The majority of patients with insulinomas experience hypoglycemic events due to uncontrolled insulin secretion. To date, surgery is the only curative treatment. However, in approximately 10% of the cases, patients have multiple lesions or metastatic disease, hampering successful surgical intervention (*2*). Therefore, preoperative localization of the lesions is critical.

Since insulinomas are typically very small (<1 cm), conventional imaging methods as MR imaging, CT, or endoscopic ultrasound, often experience difficulties to exactly localize the smallest lesions (*3*). Through the development of radiolabeled peptide ligands, such as somatostatin analogues, nuclear imaging techniques have now become available to detect small insulinoma lesions with a higher sensitivity compared to conventional techniques (*4–7*). Diagnosis can be followed by personalized treatment using these analogs, labeled with e.g. yttrium-90 or lutetium-177 (*8*). Encouraging clinical results (*8–11*) advocate somatostatin peptide receptor radionuclide therapy (PRRT) as an alternative treatment strategy for patients with unresectable or metastatic insulinomas (*10*,*12*,*13*).

However, in about 40% of the benign and 30% of the malignant insulinomas, the expression of the somatostatin receptor is absent or too low for efficient targeting (*11*,*14*). Interestingly, most somatostatin receptor negative insulinomas do express the glucagon-like peptide-1 receptor (GLP-1R), often in high density (*11*). Several studies have demonstrated the feasibility to target GLP-1R with radiolabeled exendin-4 (*6*,*11*,*15–17*), a synthetic, metabolically more stable peptide analogue of GLP-1. However, a critical concern remains the high kidney uptake. This concern is twofold: as the tail of the pancreas is in close proximity to the left kidney, localization and quantification of radiolabeled exendin-4 in the tail is hampered due

to signal spillover from the left kidney; and the high kidney uptake limits the applicability of exendin-4 for PRRT.

One approach to reduce renal accumulation of radiolabeled peptides, is to infuse succinylated gelatin (Gelofusine) (*18*). In preclinical animal models, Gelofusine efficiently reduced the renal accumulation of radiolabeled peptides, including exendin (*19*,*20*). The goal of this study was to investigate whether Gelofusine can also reduce the renal uptake of ^{111}In-labeled exendin-4 in humans and to perform dosimetric calculations to estimate the impact of Gelofusine on kidney, islet and tumor radiation dose. With this data we aimed to estimate the maximum radiation dose that could be safely administered without causing radiotoxicity to normal organs when labeled with lutetium-177.

MATERIALS AND METHODS

Subjects

Eleven healthy volunteers were recruited for this study (5 men, 6 women), of whom one female participant withdrew consent. Participants were eligible when >18 years old, with a percentage of glycated hemoglobin (HbA_{1c}) of ≤ 7%, and a normal renal function (creatinine clearance >90 mL/min by the Cockcroft and Gault formula). Exclusion criteria included heart or liver failure, hypertension, pregnancy, lactation, known hypersensitivity to Gelofusine or exendin, or a history of anaphylaxis. Written informed consent was obtained from all study participants in accordance with provisions of the Declaration of Helsinki, and the study was approved by the Institutional Ethics Review Board of the Radboud university medical center (ClinicalTrials.gov number: NCT02541734). Patient characteristics are listed in Supplemental Table 1.

Study Design

To study the effect of succinylated gelatin (Gelofusine (GELO), Braun, Oss, The Netherlands) on the renal accumulation of ^{111}In-labeled exendin-4, we performed a controlled cross-over trial with two arms (Figure 1). For each arm, two series of measurements were obtained; an ^{111}In-labeled [Lys^{40}(Ahx-DTPA)]exendin-4 SPECT/CT with saline (0.9% NaCl) (SALINE) and an ^{111}In-labeled exendin-4 SPECT/CT with Gelofusine (GELO).

^{111}In-labeled [Lys^{40}(Ahx-DTPA)]exendin-4 was prepared as previously described (*16*). The day prior to imaging, participants were asked to drink at least 2 L of water and avoid the consumption of coffee, cola, and tea. Subjects fasted for at least 4 h before ^{111}In-labeled [Lys^{40}(Ahx-DTPA)]exendin-4 injection (50MBq). Blood pressure and heart rate were monitored prior to, and 5, 15, 30, 60, 120, 180, and 240 min after infusion. Blood samples were obtained from an intravenous catheter in the contralateral arm at 2, 10, 20, 40 min before and at 1, 2, 3, and 24 h after injection. Urine was collected for 24 h in two 3-h intervals, followed by a 6- and 12-h interval. Radioactivity in blood and urine was measured with an automatic γ-counter (2480-Wizard; Perkin-Elmer, Groningen, The Netherlands). Blood glucose was measured prior to, and 15 min after tracer injection.

SPECT Acquisition and Reconstruction

24 h after tracer injection, SPECT images were acquired using an integrated SPECT/CT scanner (Symbia T16, Siemens Healthcare, IL, USA) and reconstructed as described previously (*16*). A fixed radius of rotation (25 cm) and bed height (12 cm) was applied.

Image Analysis

To determine the kidney uptake, a threshold-based volume of interest (VOI) was drawn around the kidneys in the SALINE scan, including 80% of the hottest voxels, using the Inveon Research Workplace software (Siemens Inc, Munich,

Germany). This same VOI was used to determine the kidney uptake in the GELO scan.

To determine pancreatic uptake, 2 small spherical VOIs were drawn in the pancreas as described previously (*16*). The pancreatic uptake was presented as the mean of the counts/mm^3 of both VOIs. For background correction, identical VOIs were placed in the liver.

Dosimetric Calculations

To investigate the potential of ^{177}Lu-labeled exendin for insulinoma treatment, dosimetric calculations were performed using our macro- and small scale-dosimetry model (*21*). The time integrated activity coefficients (TIAC) and dose rate S-values of the kidneys, pancreas, islets and the remainder of the body were determined previously (*21*). These values were corrected for the longer half-life of lutetium-177 as compared to indium-111, assuming similar biodistribution of the ^{111}In- and ^{177}Lu-labeled compound. As previously described (*21*), for the macro- and small scale-dosimetry model the average TIAC of five healthy volunteers was used as input. For simulation of humans with "high" or "low" kidney uptake, the maximum and minimum TIAC of these five volunteers was used, respectively.

To obtain the TIAC of insulinomas, we analyzed ^{111}In-DOTA-exendin-4 planar whole-body scintigraphic images of five patients with an insulinoma acquired at various time-points after injection (Supplemental Table 2). These scans were obtained at the university hospital in Basel, Switzerland, and have previously been published (*11*,*22*). Regions of interest were manually drawn around the insulinomas on both the anterior and posterior scans. Corresponding background regions were placed close to the regions of interest for background correction. Activity concentrations were evaluated assuming a uniform distribution in the tumor. The geometric mean obtained from the anterior and posterior views was corrected for

attenuation using the conjugate view method. The total whole body counts (geometric mean between anterior and posterior view) acquired 20 min after injection of the tracer was set as 100% injected activity, providing a "calibration factor" between counts and activity for planar recordings. The activity concentrations were expressed as percentage injected activity and corrected for the longer half-life of lutetium-177. All dosimetric evaluations were done with OLINDA/EXM software v1.1 (*23*) using the whole-body adult female and male model as well as the weighing factors recommended by the ICRP publication 60 (*23*). The area under the curve was determined, assuming only physical decay after the last measured time point. The insulinoma absorbed dose was calculated using the sphere model of OLINDA/EXM (*24*). Tumor mass was estimated based on diameter measurements, assuming a tumor density of 1 g/cm^3.

The maximum absorbed dose that could be safely delivered to the insulinoma without causing radiotoxicity to normal organs was defined as the dose that would lead to a maximum absorbed kidney dose of 23 Gy (*25*).

Statistical Analysis

Statistical analyses were performed using SPSS v.22 (SPSS, Chicago, IL, USA). Results were presented as mean ± standard deviation (SD). P-values<0.05 were considered statistically significant. An a priori power analysis was performed for the primary outcome measure (kidney uptake) based on our previous (pre)clinical studies using ^{111}In-labeled exendin-4 (*16*,*19*,*26*). A decrease in anticipated kidney uptake of 10% was considered clinically relevant. Two groups of 10 participants each would allow a statistical power of 0.80 (paired data, SD=10%, α=0.05, ρ=0.5). After data collection, normality of the distributions was assessed using the Shapiro-Wilk test. Between-group differences were analyzed by ANOVA. Differences in organ uptake between SALINE and GELO scans were analyzed using GLM univariate

repeated-measures procedures with GELO and SALINE as the within-subject factor and the sequence of the scans as the between-subject factor. The activity curves of the blood and urine were analyzed with mixed-model ANOVA with Bonferroni post-hoc test.

RESULTS

Gelofusine Significantly Reduces Kidney Uptake of Radiolabeled Exendin-4

To determine whether co-administration of GELO could significantly reduce the kidney uptake of ^{111}In-labeled exendin-4, ten healthy subjects were assigned to one of two groups (SALINE-GELO or GELO-SALINE) in a crossover design. Relevant parameters as creatinine clearance and HbA_{1c} did not significantly differ between both groups (p=0.4 and p=0.6, respectively). The infusion of saline, Gelofusine and exendin did not cause any side effects.

Representative ^{111}In-labeled exendin-4 SPECT/CT scans of the kidneys and pancreas are depicted in Figure 2A-B, 2D-E with three-dimensional projections shown in Figure 2C,F. In all subjects, infusion of Gelofusine reduced the renal uptake of ^{111}In-labeled exendin-4 (Figure 2G) ($F_{1,8}$=136.9, p=0.000003) with a mean reduction of 18.1 ± 4.2%, whereas the activity concentration in the pancreas remained unchanged ($F_{1,8}$=1.196, p=0.3) (Figure 2H). In 3 out of 10 subjects, the kidney uptake was reduced to such an extent that the pancreatic tail could be more clearly discriminated from the kidney signal (Figure 2C,F). There was no evidence that the sequence of saline or Gelofusine infusion had an effect on this outcome ($F_{1,8}$=0.102, p=0.8). Parallel to the reduction in kidney uptake, we observed a significantly higher cumulative excretion of ^{111}In-labeled exendin-4 in the urine after Gelofusine infusion (Figure 2I). The blood clearance of ^{111}In-labeled exendin-4 was significantly reduced in the first ten minutes when co-infused with Gelofusine (Figure 2J), but this did not influence pancreatic uptake.

Gelofusine Potentiates Higher Exendin Injection Dose

As the GLP-1 receptor is abundantly expressed in most insulinomas (*14*), we hypothesized that exendin may be a suitable candidate for PRRT when labeled with

lutetium-177. To estimate the radiation dose that can be delivered to insulinomas using ^{177}Lu-labeled exendin, we determined the TIAC of benign and malignant insulinomas based on planar scintigraphic images of five patients after injection with either ^{111}In-DOTA- or ^{111}In-DTPA-exendin-4 (Supplemental Table 2 and Table 1). The conversion of ^{111}In-labeled exendin-4 to ^{177}Lu-labeled exendin-4 was conducted under the assumption that the biodistribution pattern of the tracer is not affected by chelator or radiometal cation type. Based on the TIAC of the kidneys, pancreas and islets previously reported (*21*), we could estimate the tumor and islet radiation dose using our macro- and small scale-dosimetry model (*21*).

Since the kidneys are the dose-limiting organs in case of exendin (*21*), we calculated the highest activity that could be administered, and the concomitant absorbed insulinoma and islet doses that would result in the maximum allowed absorbed kidney dose of 23 Gy (*25*) for a male or female with a "low" or "high" kidney uptake (Table 1). For simulation with "high" or "low" kidney uptake, the maximum and minimum observed TIAC of the kidneys was used, respectively. In the most favorable situation (male with a low kidney uptake), the maximum activity that could be administered was 1.79 GBq, resulting in an absorbed insulinoma dose ranging from 54.2 Gy to 127.8 Gy. In the least favorable situation (female with a high kidney uptake), the injection activity could only be 1.04 GBq with a concomitant absorbed dose ranging from 30.3 Gy to 74.1 Gy (Table 1). The maximum absorbed islet radiation dose (diameter islets: 400 µm) varied between 2.6 and 4.8 Gy.

As Gelofusine effectively reduced the kidney uptake of ^{111}In-labeled exendin, protection of the kidneys allows a higher maximum injection activity. If we assume that the observed reduction would be similar for ^{177}Lu-labeled exendin and that Gelofusine does not interfere with the activity accumulation in other tissues, the maximum activity that could be injected was 2.18 GBq (Table 1). In these cases, the

highest estimated absorbed insulinoma dose would be 156.1 Gy and the maximum islet dose would remain below 5.9 Gy (Table 1).

DISCUSSION

In line with previous results in rodents (*19*,*20*,*29*), we now demonstrate that Gelofusine can substantially reduce the renal accumulation of ^{111}In-labeled [Lys^{40}(Ahx-DTPA)]exendin-4 in humans. With a mean reduction of 18.1%, the kidney uptake becomes sufficiently low to better discriminate the pancreatic tail from the kidney signal. This reduction does not only allow more accurate analyses of GLP-1R expression in the tail region of the pancreas, but it also potentiates the safe delivery of a higher radiation dose to GLP-1R positive tumors in case of PRRT.

PRRT is considered an alternative therapy in case of unresectable, or multifocal insulinomas with metastasis. Even if complete remission would not be feasible, this therapy could improve progression-free and overall survival, normalize blood glucose levels and prevent recurrent episodes of severe hypoglycemia. Our preliminary estimation of the insulinoma absorbed dose predicts a dose between 30.3 and 127.8 Gy can be safely delivered to the insulinoma; an absorbed dose range shown to induce tumor shrinkage in pancreatic neuroendocrine tumors treated with ^{177}Lu-labeled DOTATATE (*34*). Here we show this dose could be further enhanced when Gelofusine is used to protect the kidneys.

An important factor often neglected is the islet absorbed dose. Reports usually present the pancreatic absorbed dose (*35*), but since this approximation assumes homogeneous tracer distribution, this dose underestimates the radiation dose to the islets of Langerhans. Using our dedicated macro- and small scale- dosimetry model (*21*), we estimated that the islet absorbed dose for islets with a diameter of 400 µm would be below 5.9 Gy. As most human islets have a diameter between 50 and 100

μm (*36*), the islet absorbed dose for most islets would be lower. Although the exact radiation dose causing islet damage is unknown, we do know that 4.6% of the children who received a pancreatic dose of 4.4 ± 8.7 Gy with radiation therapy developed diabetes by the age of 45 years (*37*). As most insulinoma patients are adults, we believe that the risk to develop diabetes is sufficiently low, especially considering the potentially life-threatening symptoms if the insulinomas can not be surgically removed.

The only other study that performed dosimetric estimations for ^{177}Lu-labeled exendin, reports an absorbed insulinoma dose of 0.70 mGy/MBq with a maximum administrable activity of 3.7 GBq (*35*). This is in marked contrast with our observation that the insulinoma dose varies between 29.3 – 71.6 mGy/MBq with a maximum administrable activity between 1.04 – 1.79 GBq. The discrepancy between both studies may be explained, at least to some extent, by methodological differences.

First of all, the reported time-integrated activity coefficients determined by Velikyan et al. were based on biodistribution studies of ^{177}Lu-DO3A-VS-Cys40-Exendin-4 in rats which were extrapolated to the human setting, and one ^{68}Ga-DO3A-VS-Cys40-Exendin-4 PET/CT scan in a patient for the quantification of the insulinoma dose. However, it has been reported for other radiolabels that extrapolated rat data underestimates the TIAC of the kidneys by a factor of 1.8 (*38*), which could explain why Velikyan et al. report a higher tolerated activity dose. Also other time-points have been used to estimate the TIAC. In our case the last planar scintigraphic image was taken either 70 or 120 h after injection, whereas Velikyan et al. performed rat biodistribution studies up to 336 h after injection (*35*). After the last time-points both studies assumed that further decline in radioactivity occurs due to physical decay without further biological clearance. Therefore, our TIAC may even

be overestimated, underestimating the radioactivity dose that can be safely administered.

Secondly, the chelator and radiolabel vary between both studies. For the dosimetric calculations in our study, the data was only corrected for the longer half-life of lutetium-177. Based on studies that directly compared biodistribution characteristics of peptides functionalized with different chelators and labeled with various isotopes, we know that both the chelator (*39*–*41*) and the radiolabel (*41*,*42*) can influence the receptor affinity and biodistribution features of the tracer, which may explain the differences reported in both studies. However, since our preclinical studies demonstrate that the use of chelators as DTPA and DOTA, a potential chelator for lutetium-177 (*43*), does not affect the biodistribution of exendin, we assumed similar biodistribution characteristics between DOTA- and DTPA-exendin tracers in humans.

Thirdly, we estimated the absorbed insulinoma dose based on whole-body planar images, whereas the results of Velikyan et al. were based on a ^{68}Ga-exendin PET scan (*35*). As planar imaging detects radiation emanating from activity at all depths of the subject, the tumor, as well as surrounding background tissue, contribute to the detected counts. Although the background uptake of radiolabeled exendin is low, we potentially overestimated the absorbed insulinoma dose.

The predicted insulinoma absorbed dose we describe here closely resembles the dose range previously shown to successfully treat pancreatic neuroendocrine tumors with ^{177}Lu-labeled DOTATATE (*34*). These initial results suggest that GLP-1R targeting may be an interesting treatment strategy for patients with unresectable or metastatic insulinomas that are somatostatin receptor negative, especially since most somatostatin receptor negative insulinomas do express GLP1R (*11*). However, given the high inter-patient variability in GLP-1R expression (*11*,*14*), insulinoma size, and kidney uptake (*21*), we do recognize that the absorbed tumor and organ doses

may vary considerably between individuals and studies with low-dose ^{177}Lu-labeled exendin-4 are warranted to extend these preliminary observations.

CONCLUSION

Gelofusine substantially reduces the renal accumulation of radiolabeled exendin-4 in humans, potentiating the safe administration of clinically relevant injection activities for exendin-based PRRT.

DISCLOSURE

This work is supported by BetaCure (FP7/2014–2018, grant agreement 602812) and INNODIA (IMI2-JU, grant agreement 115797). MartinB and MG declare that they are an inventor and holder of the patent "Invention affecting GLP-1 and exendin" (Philipps-Universität Marburg, June 17, 2009). All other authors declare they have no conflicts of interest.

REFERENCES

1. Grant CS. Insulinoma. *Best Pract Res Clin Gastroenterol*. 2005;19:783-798.
2. Hafezi M, Fischer L, Dirlewanger A, Werner J, Buechler MW, Mehrabi A. A systematic review of localization, surgical treatment options and outcome of insulinoma. *Pancreas*. 2012;41:1363-1363.
3. Placzkowski KA, Vella A, Thompson GB, et al. Secular trends in the presentation and management of functioning insulinoma at the mayo clinic, 1987-2007. *J Clin Endocrinol Metab*. 2009;94:1069-1073.
4. Maecke HR, Hofmann M, Haberkorn U. 68Ga-labeled peptides in tumor imaging. *J Nucl Med*. 2005;46:172S-178.
5. Frilling A, Sotiropoulos GC, Radtke A, et al. The Impact of 68Ga-DOTATOC positron emission tomography/computed tomography on the multimodal management of patients with neuroendocrine tumors. *Ann Surg*. 2010;252:850-856.
6. Eriksson O, Velikyan I, Selvaraju RK, et al. Detection of metastatic insulinoma by positron emission tomography with [68Ga]exendin-4-A case report. *J Clin Endocrinol Metab*. 2014;99:1519-1524.
7. Christ E, Wild D, Ederer S, et al. Glucagon-like peptide-1 receptor imaging for the localisation of insulinomas: a prospective multicentre imaging study. *Lancet Diabetes Endocrinol*. 2013;1:115-122.
8. Brabander T, Teunissen JJM, Van Eijck CHJ, et al. Peptide receptor radionuclide therapy of neuroendocrine tumours. *Best Pract Res Clin Endocrinol Metab*. 2016;30:103-114.
9. Imhof A, Brunner P, Marincek N, et al. Response, survival, and long-term toxicity after therapy with the radiolabeled somatostatin analogue [90Y-DOTA]-TOC in metastasized neuroendocrine cancers. *J Clin Oncol*.

2011;29:2416-2423.

10. Kwekkeboom DJ, De Herder WW, Kam BL, et al. Treatment with the radiolabeled somatostatin analog [177Lu- DOTA0,Tyr3]octreotate: Toxicity, efficacy, and survival. *J Clin Oncol*. 2008;26:2124-2130.
11. Wild D, Christ E, Caplin ME, et al. Glucagon-like peptide-1 versus somatostatin receptor targeting reveals 2 distinct forms of malignant insulinomas. *J Nucl Med*. 2011;52:1073-8.
12. Ezziddin S, Khalaf F, Vanezi M, et al. Outcome of peptide receptor radionuclide therapy with 177Lu-octreotate in advanced grade 1/2 pancreatic neuroendocrine tumours. *Eur J Nucl Med Mol Imaging*. 2014;41:925-33.
13. Kam BLR, Teunissen JJM, Krenning EP, et al. Lutetium-labelled peptides for therapy of neuroendocrine tumours. *Eur J Nucl Med Mol Imaging*. 2012;39:S109-S112.
14. Reubi JC, Waser B. Concomitant expression of several peptide receptors in neuroendocrine tumours: molecular basis for in vivo multireceptor tumour targeting. *Eur J Nucl Med Mol Imaging*. 2003;30:781-793.
15. Brom M, Joosten L, Frielink C, Boerman O, Gotthardt M. 111In-exendin Uptake in the Pancreas Correlates With the β-Cell Mass and Not With the α-Cell Mass. *Diabetes*. 2015;64:1324-1328.
16. Brom M, Woliner-van der Weg W, Joosten L, et al. Non-invasive quantification of the beta cell mass by SPECT with (111)In-labelled exendin. *Diabetologia*. 2014;57:950-959.
17. Wicki A, Wild D, Storch D, et al. [Lys40(Ahx-DTPA-111In)NH2]-exendin-4 is a highly efficient radiotherapeutic for glucagon-like peptide-1 receptor-targeted therapy for insulinoma. *Clin Cancer Res*. 2007;13:3696-3705.
18. Veldman BAJ, Schepkens HLE, Vervoort G, Klasen I, Wetzels JFM. Low concentrations of intravenous polygelines promote low-molecular weight

proteinuria. *Eur J Clin Invest*. 2003;33:962-968.

19. Vegt E, Eek A, Oyen WJG, de Jong M, Gotthardt M, Boerman OC. Albumin-derived peptides efficiently reduce renal uptake of radiolabelled peptides. *Eur J Nucl Med Mol Imaging*. 2010;37:226-34.
20. Vegt E, van Eerd JEM, Eek A, et al. Reducing renal uptake of radiolabeled peptides using albumin fragments. *J Nucl Med*. 2008;49:1506-11.
21. van der Kroon I, Woliner-van der Weg W, Brom M, et al. Whole organ and islet of Langerhans dosimetry for calculation of absorbed doses resulting from imaging with radiolabeled exendin. *Sci Rep*. 2017;7:39800.
22. Christ E, Wild D, Forrer F, et al. Glucagon-like peptide-1 receptor imaging for localization of insulinomas. *J Clin Endocrinol Metab*. 2009;94:4398-405.
23. Stabin MG, Sparks RB, Crowe E. OLINDA/EXM: The Second-Generation Personal Computer Software for Internal Dose Assessment in Nuclear Medicine. *J Nucl Med*. 2005;46:1023-1027.
24. Stabin MG, Komjnenberg MW. Re-Evaluation of Absorbed Fractions for Photons and Electrons in Spheres of Various Sizes. *J Nucl Med*. 2000;41:149-160.
25. Dawson LA, Kavanagh BD, Paulino AC, et al. Radiation-Associated Kidney Injury. *Int J Radiat Oncol Biol Phys*. 2010;76:108-115.
26. Rylova SN, Waser B, Del Pozzo L, et al. Approaches to improve the pharmacokinetics of radiolabeled glucagon-like peptide-1 receptor ligands using antagonistic tracers. *J Nucl Med*. 2016;57:1282-1288.
27. Läppchen T, Tönnesmann R, Eersels J, Meyer PT, Maecke HR, Rylova SN. Radioiodinated exendin-4 is superior to the radiometal-labelled glucagon-like peptide-1 receptor probes overcoming their high kidney uptake. *PLoS One*. 2017;12:e0170435.
28. Mikkola K, Yim C, Lehtiniemi P, et al. Low kidney uptake of GLP-1R-targeting , beta cell-specific PET tracer , 18 F-labeled promise for clinical imaging.

EJNMMI Res. 2016;6:1-11.

29. Gotthardt M, van Eerd-Vismale J, Oyen WJG, et al. Indication for different mechanisms of kidney uptake of radiolabeled peptides. *J Nucl Med*. 2007;48:596-601.
30. Zaknun JJ, Bodei L, Mueller-Brand J, et al. The joint IAEA, EANM, and SNMMI practical guidance on peptide receptor radionuclide therapy (PRRNT) in neuroendocrine tumours. *Eur J Nucl Med Mol Imaging*. 2013;40:800-816.
31. Rolleman EJ, Melis M, Valkema R, Boerman OC, Krenning EP, De Jong M. Kidney protection during peptide receptor radionuclide therapy with somatostatin analogues. *Eur J Nucl Med Mol Imaging*. 2010;37:1018-1031.
32. Vegt E, Wetzels JFM, Russel FGM, et al. Renal uptake of radiolabeled Octreotide in human dubjects is efficiently inhibited by succinylated gelatin. *J Nucl Med*. 2006;47:432-436.
33. Gotthardt M, van Eerd-Vismale J, Oyen WJG, et al. Indication for different mechanisms of Kidney Uptake of Radiolabeled Peptides. *J Nucl Med*. 2007;48:596-601.
34. Ilan E, Sandstrom M, Wassberg C, et al. Dose response of pancreatic neuroendocrine tumors treated with peptide receptor radionuclide therapy using 177Lu-DOTATATE. *J Nucl Med*. 2015;56:177-182.
35. Velikyan I, Bulenga TN, Selvaraju R, et al. Dosimetry of [177lu]-do3a-vs-cys40-exendin-4-impact on the feasibility of insulinoma internal radiotherapy. *Am J Nucl Med Mol Imaging*. 2015;5:109-126.
36. Kilimnik G, Jo J, Periwal V, Zielinski MC, Hara M. Quantification of islet size and architecture. *Islets*. 2012;4:167-172.
37. de Vathaire F, El-Fayech C, Ben Ayed FF, et al. Radiation dose to the pancreas and risk of diabetes mellitus in childhood cancer survivors: A retrospective cohort study. *Lancet Oncol*. 2012;13:1002-1010.

38. Selvaraju RK, Bulenga TN, Espes D, Lubberink M, Sörensen J. Dosimetry of [68Ga]-Ga-D03A-VS-Cys40-Exendin-4 in rodents, pigs , non-human primates and human - repeated scanning in human is possible. 2015;5:259-269.
39. Fani M, Del Pozzo L, Abiraj K, et al. PET of somatostatin receptor-positive tumors using 64Cu- and 68Ga-somatostatin antagonists: the chelate makes the difference. *J Nucl Med*. 2011;52:1110-1118.
40. Kwekkeboom DJ, Kooij PP, Bakker WH, Mäcke HR, Krenning EP. Comparison of 111In-DOTA-Tyr3-octreotide and 111In-DTPA-octreotide in the same patients: biodistribution, kinetics, organ and tumor uptake. *J Nucl Med*. 1999;40:762-767.
41. Reubi JC, Schär J-C, Waser B, et al. Affinity profiles for human somatostatin receptor subtypes SST1-SST5 of somatostatin radiotracers selected for scintigraphic and radiotherapeutic use. *Eur J Nucl Med Mol Imaging*. 2000;27:273-282.
42. Bauman A, Valverde IE, Fischer CA, Vomstein S, Mindt TL. Development of 68 Ga-and 89 Zr-Labeled Exendin-4 as Potential Radiotracers for the Imaging of Insulinomas by PET. *J Nucl Med*. 2015;56:1569-1574.
43. Stimmel JB, Kull FC. Samarium-153 and Lutetium-177 chelation properties of selected macrocyclic and acyclic ligands. *Nucl Med Biol*. 1998;25:117-125.

Tables

Table 1: Dosimetry calculations for ^{177}Lu-labeled exendin

		Low kidney uptake										High kidney uptake									
		Patient1		Patient2		Patient3		Patient4		Patient5		Patient1		Patient2		Patient3		Patient4		Patient5	
		M	F	M	F	M	F	M	F	M	F	M	F	M	F	M	F	M	F	M	F
	TIAC insulinoma (h)	0.44	0.44	0.81	0.81	0.65	0.65	0.62	0.62	0.96	0.96	0.44	0.44	0.81	0.81	0.65	0.65	0.62	0.62	0.96	0.96
	Kidney dose (Gy)	23	23	23	23	23	23	23	23	23	23	23	23	23	23	23	23	23	23	23	23
Without Gelofusine	Max. inj. activity (GBq)	1.79	1.64	1.79	1.64	1.79	1.64	1.79	1.64	1.79	1.64	1.12	1.04	1.12	1.04	1.12	1.04	1.12	1.04	1.12	1.04
	Insulinoma dose (Gy)	127.8	117.4	54.2	48.0	90	82.7	78.5	72.2	112.2	103.1	80.2	74.1	32.9	30.3	56.5	52.2	49.3	45.5	70.7	65.1
	Islet dose (Gy)	4.0	4.8	4.0	4.8	4.0	4.8	4.0	4.8	4.0	4.8	2.6	3.0	2.6	3.0	2.6	3.0	2.6	3.0	2.6	3.0
With Gelofusine	Max. inj. activity (GBq)	2.18	2.01	2.18	2.01	2.18	2.01	2.18	2.01	2.18	2.01	1.38	1.26	1.38	1.26	1.38	1.26	1.38	1.26	1.38	1.26
	Insulinoma dose (Gy)	156.1	143.6	63.8	58.7	109.9	101.1	95.9	88.2	137.0	126.0	98.5	90.2	40.2	36.9	69.3	63.5	60.5	55.4	86.4	79.2
	Islet dose (Gy)	4.9	5.8	4.9	5.8	4.9	5.8	4.9	5.8	4.9	5.8	3.1	3.7	3.1	3.7	3.1	3.7	3.1	3.7	3.1	3.7

(M=male, F=female, input parameters for the model: islet size: 400 μm, percentage of islets in the pancreas: 2%).

Figures

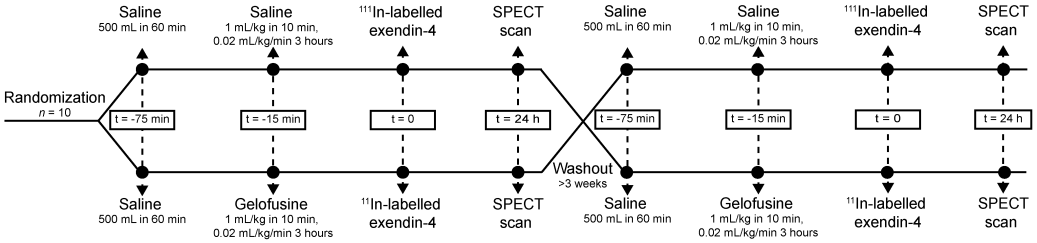

Figure 1. Time-line of the cross-over trial

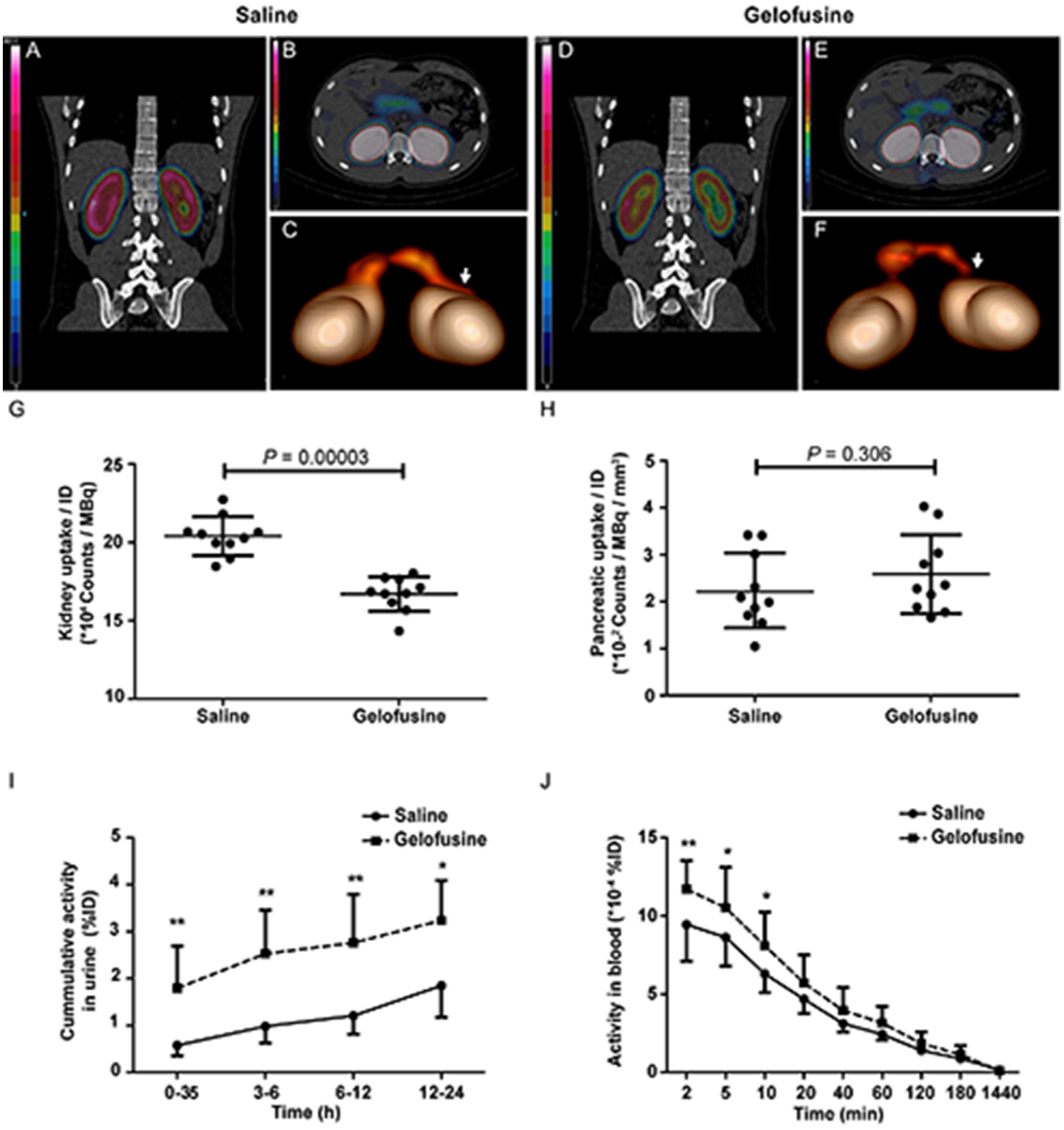

Figure 2. Quantitative analysis of kidney and pancreatic uptake of ^{111}In-labeled exendin-4 in SPECT/CT scans. SPECT/CT images (A,B,D,E) were obtained 24 hours after ^{111}In-exendin injection, co-infused with saline (A,B) or Gelofusine (D, E). In 3 out of 10 patients, 3D projections of the SPECT images (C, F) demonstrated that the pancreas could be more clearly discriminated from the kidney signal after Gelofusine injection (white arrow) (F). Kidney uptake of ^{111}In-labeled exendin-4 was significantly reduced after administration Gelofusine (G) whereas the activity concentration in the

pancreas remained the same (H). Clearance of ^{111}In-labeled exendin-4 was determined in the urine (I) and in the blood (J). *p<0.05, **p<0.01.

Supplemental table 1: Characteristics of healthy volunteers

	SALINE-GELO	GELO-SALINE
Age (years)	29.0 ± 9.3	19.8 ± 0.4
Sex (m/f)	3/2	2/3
BMI (kg/m^2)	21.4 ± 1.4	20.3 ± 3.4
HbA1c (mmol/mol)	34.6 ± 1.9	35.2 ± 2.0
Creatine clearance (cc/min)	116 ± 27	106 ± 15

Supplemental table 2: Characteristics of insulinoma patients

	Insulinoma type	Tumor Ø (mm)	Scan time (h)	Tracer	Injection dose (MBq(ug))
Patient1	Benign	10	0.33, 4, 22, 70	DOTA-exendin	89(30)
Patient2	Benign	17	0.25, 3.5, 24, 70	DOTA-exendin	97(30)
Patient3	Benign	13	0.33, 3.5, 96 90/30	DOTA-exendin	90(30)
Patient4	Malignant	15	0.25, 3.5, 22, 120	DOTA-exendin	145(20)
Patient5	Malignant	14	0.25, 3.5, 21.5,120	DTPA-exendin	145(10)